Finite Element Modeling And Parametric Optimization of Solidly Mounted Film Bulk Acoustic Resonator For Its Performance Enhancement

Arun Kishor Johar (2015rec9018@mnit.ac.in)
MNIT Jaipur: Malaviya National Institute of Technology https://orcid.org/0000-0002-3367-9828
Jai Kumar Bhatt
MNIT Jaipur: Malaviya National Institute of Technology
Gaurav Kumar Sharma
GLA University Mathura
Tangudu Bharat Kumar
MNIT Jaipur: Malaviya National Institute of Technology
Tarun Varma
MNIT Jaipur: Malaviya National Institute of Technology
C. Periasamy
MNIT Jaipur: Malaviya National Institute of Technology
Ajay Agarwal
CEERI Pilani: Central Electronics Engineering Research Institute CSIR
Dharmendar Boolchandani
MNIT Jaipur: Malaviya National Institute of Technology

Research Article

Keywords: Solidly mounted film bulk acoustic resonator (SMR or SMFBAR), finite element modeling (FEM), Design of Experiments (DoE), Analysis of Variance (ANOVA), coupling coefficient (Keff2), Quality factor (Q) and figure of merit (FoM)

Posted Date: August 12th, 2021

DOI: https://doi.org/10.21203/rs.3.rs-379665/v1

Finite Element Modeling and Parametric Optimization of Solidly Mounted Film Bulk Acoustic Resonator for its Performance Enhancement

Arun Kishor Johar[1, *], Jai Kumar Bhatt[1], Gaurav Kumar Sharma[2], Tangudu Bharat Kumar[1], Tarun Varma[1], C. Periasamy[1], Ajay Agarwal[3], D. Boolchandani[1]

[1]Department of Electronics & Communication Engineering, Malaviya National Institute of Technology Jaipur, Jaipur, Rajasthan - 302017, India

[2]Department of Electronics and Communication Engineering, GLA University, Mathura, Uttar Pradesh - 281406, India

[3]Nano Biosensors Group, CSIR-Central Electronics Engineering Research Institute (CEERI) Pilani, Rajasthan – 333031, India.

*corresponding author Email: 2015rec9018@mnit.ac.in, Phone (off.) :+91-1412713334, Fax: +91-1412529029,

Abstract

This paper reports, the application of Taguchi Design of Experiments (DoE) and ANOVA (Analysis of Variance) for finding the optimal combinations and analysis of the effect of individual layer thickness on the performance of SMR sensor. The optimum combination of design parameters and its performance as a sensor have been predicted with DoE and validated through the finite element modeling (FEM) simulation. The optimization has been done to achieve enhancement in coupling coefficient of SMR sensor. The best optimized thickness of metal electrodes, piezoelectric, sensing, insulation low and high acoustic impedance layers have been found to be 0.2µm, 2µm, 0.68µm, 0.3µm, 1.028µm and 1.008µm, respectively. The results of the present study show that for the optimized dimension of SMR structure, simulated values of coupling coefficient (K_{eff}^2), Quality factor (Q) and figure of merit (FoM) are 0.075596 (or 7.5596%), 1171.6 and ≈ 88, respectively. Optimized structure performance has been compared with the existing SMR sensors and it is observed that proposed SMR exhibits performance enhancement in terms of FoM by ≈ 37 %.

Keywords: *Solidly mounted film bulk acoustic resonator (SMR or SMFBAR), finite element modeling (FEM), Design of Experiments (DoE), Analysis of Variance (ANOVA), coupling coefficient (K_{eff}^2), Quality factor (Q) and figure of merit (FoM).*

Introduction

Film bulk acoustic resonators have been employed in various sensing applications because of its high sensitivity, ability to perform rapid measurements, design simplicity and lower design cost [1]. These sensors have very high accuracy and precision as compared to the capacitive and resistive sensors [2-3]. Initial development of bulk acoustic wave (BAW) devices has been started in 1980 [4]. Generally, the BAW devices have been implemented by a piezoelectric layer fixed between thin metal layers on a silicon substrate using the bulk micro-machining process [5]. The piezoelectric effect is used to produce the resonance in BAW resonators. Application of an ac electric signal to BAW device produces acoustic waves and propagation of these waves take places in the longitudinal direction to the electric field [6]. Bottom electrode is used for the measurement of longitudinal acoustic wave backside reflection. The acoustic wave confinement inside the piezoelectric layer can be achieved by perfect confinement of acoustic wave inside BAW device. Perfect confinement of the acoustic wave can be accomplished by the unity magnitude of reflection coefficient [7]. BAW resonators are broadly classified into two categories: 1. Film bulk acoustic resonator (FBAR) and 2. Solidly mounted resonator (SMR) or solidly mounted film bulk acoustic resonator (SMFBAR). Solidly mounted resonator are preferred over FBAR because of its high robustness, low risk of mechanical damage during dicing process, low layer stresses and good power handling capacity [8]. The piezoelectric layer material, its thickness and mass loading affect the resonance characteristics of the SMR. Variations in any of these parameters result in the down shifting in resonant/ anti-resonant frequency of SMR [9].

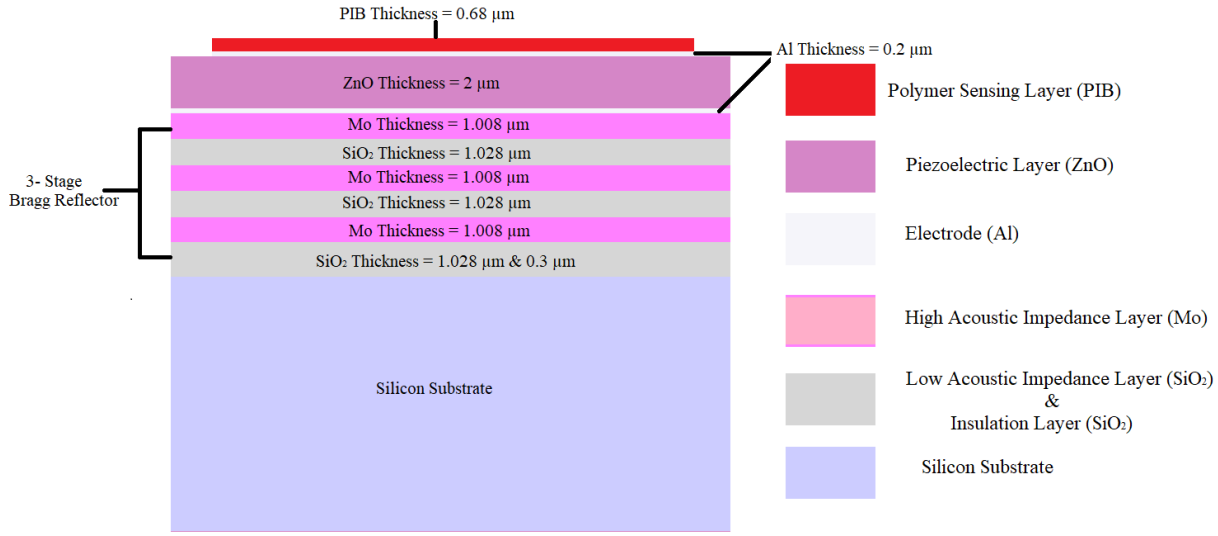

Figure 1: Proposed SMR sensor structure.

Figure 1 represents the SMR sensor structure. In SMR sensor Bragg reflector configuration provides the reflection of the acoustic waves in descending direction. Acoustic mirror is composed of high and low acoustic impedance layers (SiO_2 and Mo) [10-11]. The SiO_2 and Mo layers are stacked on one over another to form Bragg reflector. Bragg reflector with a three stage configuration has been used for proposed structure for eliminating the spurious modes, as illustrated in Figure 1. One more SiO_2 layer is used to perform function of insulating layer on Si substrate. For the proposed SMR structure ZnO has been selected as piezoelectric materials because of its fabrication process compatibility and lower fabrication cost [12-13]. Polyisobutylene (PIB) has been selected as sensing layer because its partition coefficient has been known for the most of the gases [14-15]. Aluminum has been selected as electrode material because of its simple fabrication process and low fabrication cost [16]. The essential boundary conditions for performing simulation in COMSOL Multiphysics environment are (1) Bottom electrode terminal is connected to ground where as top electrode terminal is connected to positive 1V supply, (2) SMR structure is fixed to both sides by applying fixed constraints to its both sides and (3) Appropriate perfectly matched layers (PML) must be defined for simulating the structure. The acoustic velocity and piezoelectric layer thickness are used to calculate the fundamental resonance frequency of the BAW device. The fundamental resonance frequency is given by [4]

$$f = \frac{\vartheta}{2t_p} \tag{1}$$

here, ϑ & t_p denotes the acoustic wave velocity & piezoelectric layer thickness, respectively. The equation (1) states that fundamental resonance frequency and thickness of piezoelectric layer are inversely proportional to each other in BAW devices. For SMR devices when out of phase condition is generated inside the resonator, acoustic waver suffers from both the polarizations either mechanically induced or dielectric polarizations this causes parallel resonance to takes place [4, 9]. Under parallel resonance condition, degradation in net current is observed because of net polarization. The electrical impedance (Z_{elec},) between electrodes can be obtained by application of external excitation to the SMR. Under external excitation the electrical impedance is given by [17]

$$Z_{elec} = \frac{1}{j\omega C_0}\left[1 - k_{eff}^2 \frac{tan\left(\frac{\beta t_p}{2}\right)}{\left(\frac{\beta t_p}{2}\right)}\right] \tag{2}$$

Where k_{eff}^2, ω, t_p and β denote the effective coupling coefficient, angular frequency, piezoelectric layer thickness and propagation constant, respectively. The Mason's model of

SMR sensor can be reduced to either 4 or 6 lumped elements if the ratio or electrode thickness to piezoelectric layer thickness becomes negligible [18].

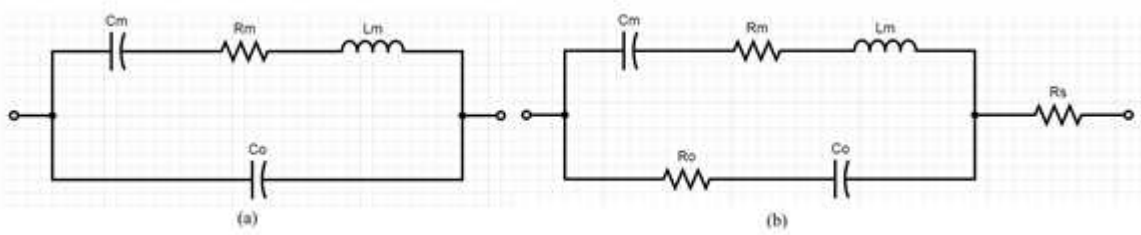

Figure 2: (a) The Butterworth-Van-Dyke (BVD) and (b) its modified BVD (mBVD) equivalent for proposed device.

The basic Butterworth-Van-Dyke (BVD) and its modified BVD (mBVD) equivalent for the proposed device are shown in figure 2 (a) and (b), respectively. In BVD and mBVD equivalent circuits R_m, C_m, L_m and C_o denotes the motional or dynamic resistance, capacitance, inductance and static capacitance, respectively. Whereas R_o denote the dielectric loss of the piezoelectric layer and R_s is the electrical loss of the two electrodes. Equations given below can be used to determine the value of these circuit elements [2,19-20]:

$$\text{Static capacitance } (C_0) = \frac{\varepsilon A}{d} \tag{3}$$

$$\text{Motional or dynamic inductance}(\mathrm{L_m}) = \frac{\pi^3 \vartheta_a}{8\varepsilon A \omega^3 k_{eff}^2} = \frac{1}{(\omega)^2 C_m} \tag{4}$$

$$\text{Motional capacitance or dynamic}(\mathrm{C_m}) = \frac{8}{\pi^2} k_{eff}^2 C_0 = C_0 \left[\left(\frac{\omega_p}{\omega}\right)^2 - 1\right] \tag{5}$$

$$\text{Motional or dynamic resistance}(\mathrm{R_m}) = \frac{\pi\eta\varepsilon}{8k_{eff}^2 \rho A \omega \vartheta_a} = \frac{1}{\omega C_m Q} \tag{6}$$

$$\omega^2 = \frac{1}{L_m C_m} \tag{7}$$

where, ω & ω_p, A, k^2_{eff} , ε, ρ, η, ϑ_a *and* d denotes the series & parallel resonant frequency, area of resonator, piezoelectric coupling coefficient permittivity, density, acoustic viscosity, acoustic velocity, thickness of piezoelectric layer, respectively. The piezoelectric coupling coefficient (k_{eff}^2) is given by equation 8 [21-23].

$$k_{eff}^2 = \frac{\pi^2}{4}\left(\frac{f_{ar} - f_r}{f_{ar}}\right) \tag{8}$$

This coupling coefficient of the FBAR device shows proportional relationship with the figure of merit (FoM) [24]. Hence, enhancement in coupling coefficient also enhances the FoM. The piezoelectric material's acoustic velocity (ϑ_a) is given by equation 9 [25]:

$$\vartheta_a = \sqrt{\frac{c_{33}^D}{\rho}} \tag{9}$$

where, c_{33}^D and ρ denote elastic stiffness at a constant electric displacement and density of piezoelectric layer, respectively. The optimization of the SMR device becomes more critical because the various layer materials and their thickness plays a key role in the SMR device performance.

Present work reports the utilization of Taguchi DoE and ANOVA (Analysis of Variance) to find the best optimized SMR dimensions and to analyze the effect of each layer thickness on performance of the sensor. Statistical optimization methods of Taguchi and ANOVA are selected as they require less number of experiments to be performed. For a design having 3 levels for 3 factors, 27 experiments are required to be performed for attaining optimum performance which is very tedious and time-consuming process. Taguchi L9 orthogonal array simplifies above issue by reducing the number of experiments to 9 only as compared to 27 experiments [26-31]. Performance optimization of FBAR/SMR sensor using Taguchi DoE and ANOVA technique has not been reported yet, as per author's knowledge. First time Taguchi DoE and ANOVA optimization techniques are used to find the optimized dimension of SMR sensor. It is shown that how the thickness of each layer affects the sensor performance. In the proposed structure, enhanced sensitivity can be achieved by coating the top electrode with thin layer of sensitive material. The device dimensions have been optimized in two steps. First the basic FBAR has been designed then Taguchi DoE and ANOVA optimization have been performed on Insulation layer, piezoelectric layer and electrode thickness to achieve enhanced coupling coefficient.

A. Taguchi and ANOVA DoE approach to find optimum combination for coupling coefficient enhancement of simple FBAR

The performance of FBAR sensor broadly depends on three factors: 1. Electrode thickness (A), 2. Piezoelectric layer thickness (B), and 3. Insulation layer Thickness (C). These factors have been selected for the detailed analysis and to find the optimum combinations. Each of these factors (A, B, C) are assigned with the three distinct levels. Table 1, presents the factors and their levels assigned.

Table 1: Control Factors of FBAR and their levels

Control Factor	Level 1	Level 2	Level 3
Electrode Thickness (µm) (A)	0.2	0.5	0.8
Piezoelectric Layer Thickness (µm) (B)	1	1.5	2
Insulation Layer Thickness (µm) (C)	0.3	0.5	0.7

In this array 1, 2, 3 denote the levels of respective factors. In the array, all the factor levels combinations occurs equally in all columns, hence the array is orthogonal. The last column of the Table 2, represents the coupling coefficient of the sensor. Simulation was conducted 9 times and an average value is taken for say experiment i, where i =1, 2, 3, … 9 different experiments/simulation combinations. The factors, their combination and results obtained from FEM simulation on COMSOL Multiphysics software are tabulated in Table 2.

Table 2: Experiment as per L9 orthogonal array for Basic FBAR sensor.

S.No.	Control Factor			Output Parameters		
	Electrode Thickness (µm)	Piezoelectric Layer Thickness (µm)	Insulation Layer Thickness (µm)	Resonant Frequency (GHz)	Anti Resonant Frequency (GHz)	Coupling Coefficient (K_{eff}^2)
1	1	1	1	3.798	3.801	0.001945
2	1	2	2	2.236	2.248	0.013158
3	1	3	3	1.360	1.402	0.073842
4	2	1	2	3.961	3.964	0.001865
5	2	2	3	2.344	2.356	0.012555
6	2	3	1	1.213	1.249	0.071046
7	3	1	3	4.066	4.069	0.001817
8	3	2	1	2.131	2.145	0.016088
9	3	3	2	1.078	1.108	0.066739

The objective of the Taguchi method is to predict optimum conditions/combinations. The optimum combinations are indicated where the contribution of the level to deviate away from the mean. Table 3, presents the optimum levels indicated with * mark. Using the additive model, the value of coupling coefficient; under optimum combinations as,

$$K_{eff}^2 = m + (m_{A1} - m) + (m_{B3} - m) + (m_{C1} - m) \qquad = 0.075056 \qquad (10)$$

Table 3: Response Table for Means

Level	A	B	C
1	0.030315*	0.001876	0.029693*
2	0.028489	0.014600	0.027921
3	0.028215	0.070542*	0.029405
Delta	0.002100	0.068667	0.001772
Rank	2	1	3

A verification simulation is conducted after determining the optimum conditions and predicting the response with these combinations. The simulation result has been compared with the predicted value of coupling coefficient (K_{eff}^2). Predicted value of K_{eff}^2 is 0.075056 and the simulated value of K_{eff}^2 is 0.073947. Hence, it can be concluded that this model adequately determines the K_{eff}^2 in terms of defined variables.

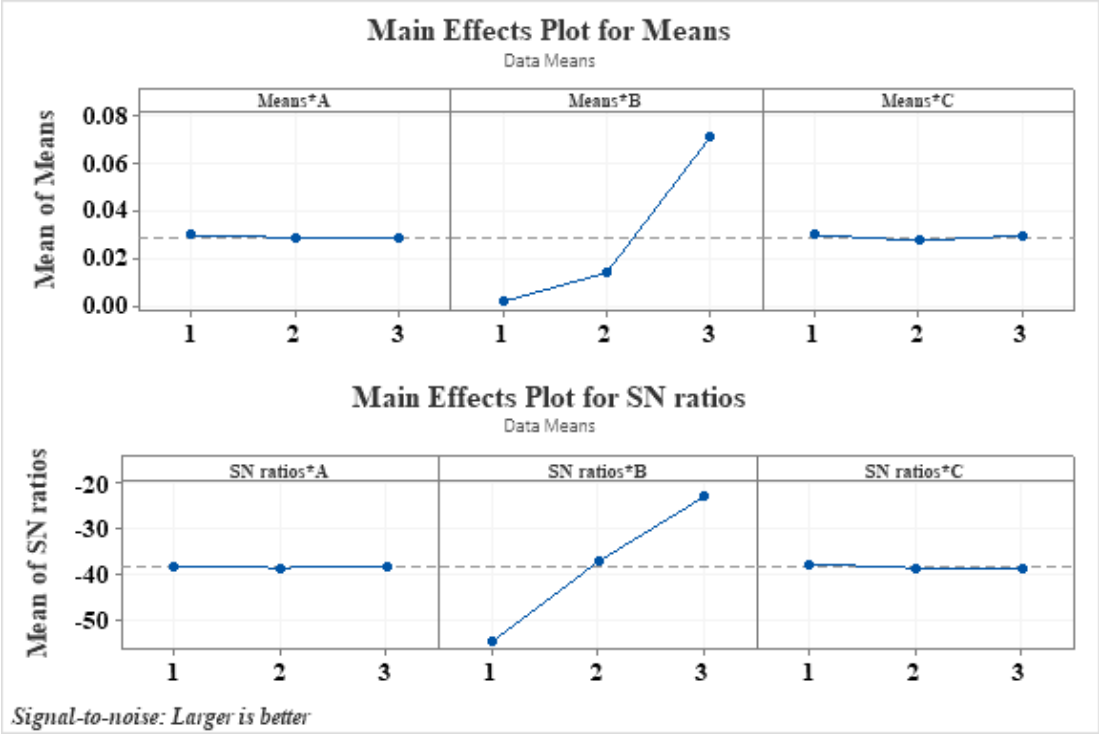

Figure 3: Main effect plot for means and SN ratios for FBAR.

Figure 3 shows, the main effect plot for means and SN Ratios obtained from Taguchi DoE Analysis using Minitab 19 Software. Figure 3 describes the effect of various levels of control factors on coupling coefficient. From the curve it can be said that, for control factor B (Piezoelectric Layer Thickness) Level 3 have significant effect on designing of FBAR sensor whereas control factor A

and C have very less effect on designing of FBAR sensor. Interaction plots of various control factors are shown in Figure 4.

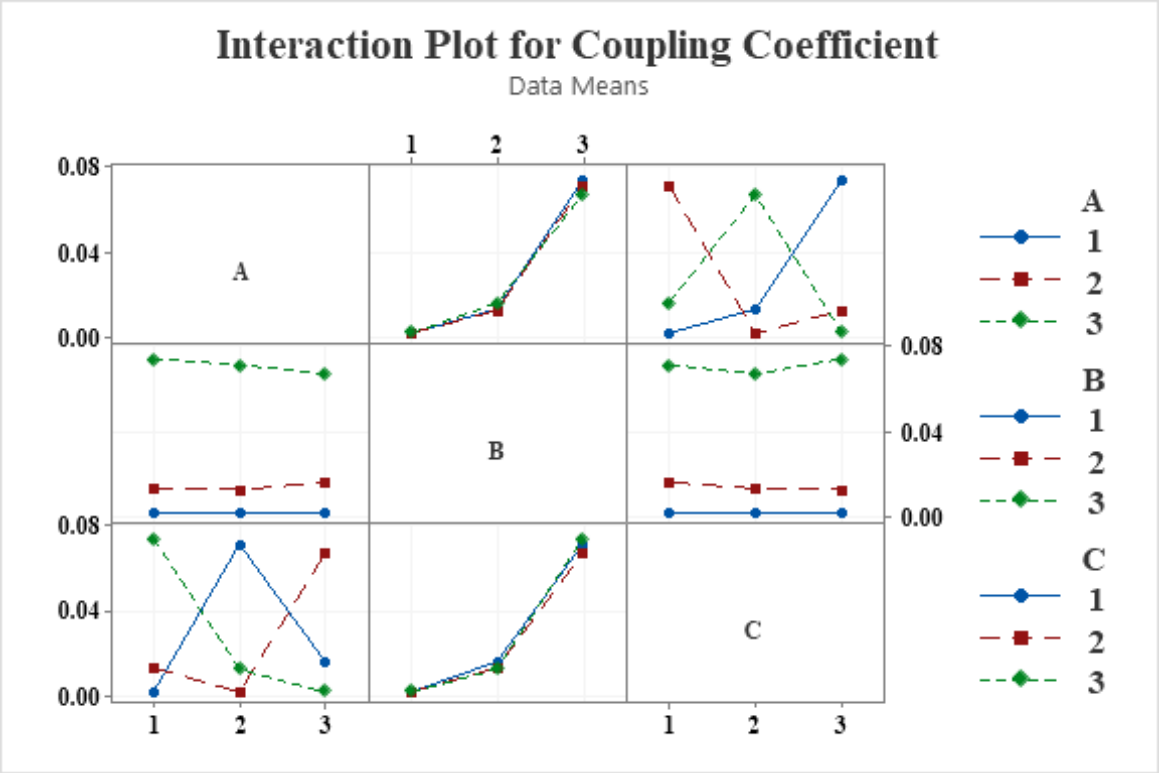

Figure 4: Interaction plot for FBAR sensor coupling coefficient

Table 4: Analysis of Variance

Factor	DoF	Sum of Squares	Mean of Squares	F-Value	P-Value
A	2	0.000008	0.000004	0.41	0.709
B	2	0.008007	0.004003	419.76	0.002
C	2	0.000005	0.000003	0.28	0.779
Error	2	0.000019	0.000010		
Total	8	0.008039			

From Table 4 which presents, Analysis of Variance, it is evident that factor A and C have very less/negligible effect on coupling coefficient of FBAR. Only factor B is responsible for variation in coupling coefficient of FBAR sensor and overall impact of Factor B on coupling coefficient is 99.8359%. Similarly effect of factors A and C have been calculated and it is observed that overall impact of Factors A and C on coupling coefficient is 0.0975 % and 0.0666%, respectively.

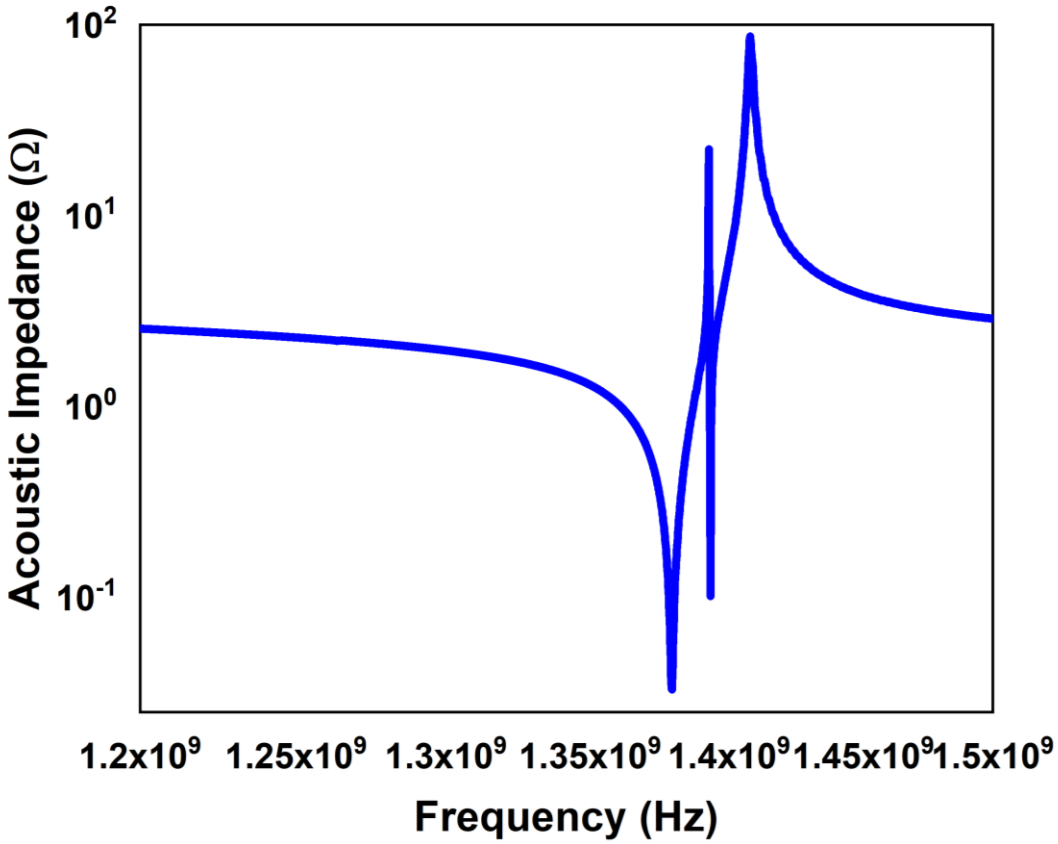

Figure 5: Acoustic Impedance v/s frequency plot for Optimized FBAR.

After that simulations were performed for optimized device. Figure 5 shows the resonance behavior of the optimized FBAR device. The spurious modes are present in the resonance characteristics of the FBAR device, as shown in Figure 5. The spurious modes are unwanted and affect the sensing performance. Therefore, the elimination of spurious modes becomes essential. As per the literature, Bragg's reflector configuration completely eliminates the spurious modes [32]. Hence, FBAR is designed with this multi layered Bragg reflector configuration and known as SMR. Now to optimize the dimensions of this SMR structure second time optimization have been done to achieve enhanced coupling coefficient.

B. Taguchi and ANOVA DoE approach to find optimum combination for coupling coefficient enhancement of proposed SMR

The performance of SMR sensor broadly depends on three factors: 1. SiO_2 low acoustic impedance layer Thickness (A). 2. Mo High acoustic impedance layer Thickness (B). 3. Sensing layer Thickness (C). These factors are selected for the detailed analysis of each factor and to find the optimum combinations. Each of these factors (A, B, C) are assigned with the three distinct levels. Table 5, presents the factors and their levels assigned.

Table 5: Control Factors of FBAR and their levels

Control Factor	Level 1	Level 2	Level 3
SiO_2 Layer Thickness in Bragg Reflector Configuration (µm) (A)	0.514	1.028	1.542
Mo Layer Thickness in Bragg Reflector Configuration (µm) (B)	0.504	1.008	1.512
Sensing Layer Thickness (µm) (C)	0.34	0.51	0.68

Table 6: Experiment as per L9 orthogonal array for proposed SMR.

S.No.	Control Factor			Output Parameters		
	SiO2 Layer Thickness in Bragg Reflector Configuration	Mo Layer Thickness in Bragg Reflector Configuration	Sensing Layer Thickness	Resonant Frequency (GHz)	Anti Resonant Frequency (GHz)	Coupling Coefficient (K^2_{eff})
1	1	1	1	1.332	1.341	0.016543
2	1	2	2	1.487	1.526	0.062995
3	1	3	3	1.433	1.472	0.065306
4	2	1	2	1.39	1.429	0.067272
5	2	2	3	1.339	1.381	0.074964
6	2	3	1	1.435	1.474	0.065218
7	3	1	3	1.267	1.306	0.073607
8	3	2	1	1.267	1.303	0.068102
9	3	3	2	1.234	1.267	0.0642

As detailed in Table 6, Simulation was conducted 9 times. The factors, their combination and results obtained from FEM simulation using COMSOL Multiphysics software are tabulated in Table 6. Table 7, presents the optimum levels indicated with * mark.

Table 7: Response Table for Means

Level	A	B	C
1	0.04828	0.05247	0.04995
2	0.06915*	0.06869*	0.06482
3	0.06864	0.06491	0.07129*
Delta	0.02087	0.01621	0.02134
Rank	2	3	1

Using the additive model, the value of coupling coefficient; under optimum combinations as,

$$K^2_{eff} = m + (m_{A2} - m) + (m_{B2} - m) + (m_{C3} - m) \ = 0.085084 \qquad (11)$$

The simulation result has been compared with the predicted value of coupling coefficient (K^2_{eff}). Predicted value of K^2_{eff} is 0.085084 and the simulated value of K^2_{eff} is 0.075596. Hence, it can be concluded that this model adequately determines the K^2_{eff} in terms of defined variables.

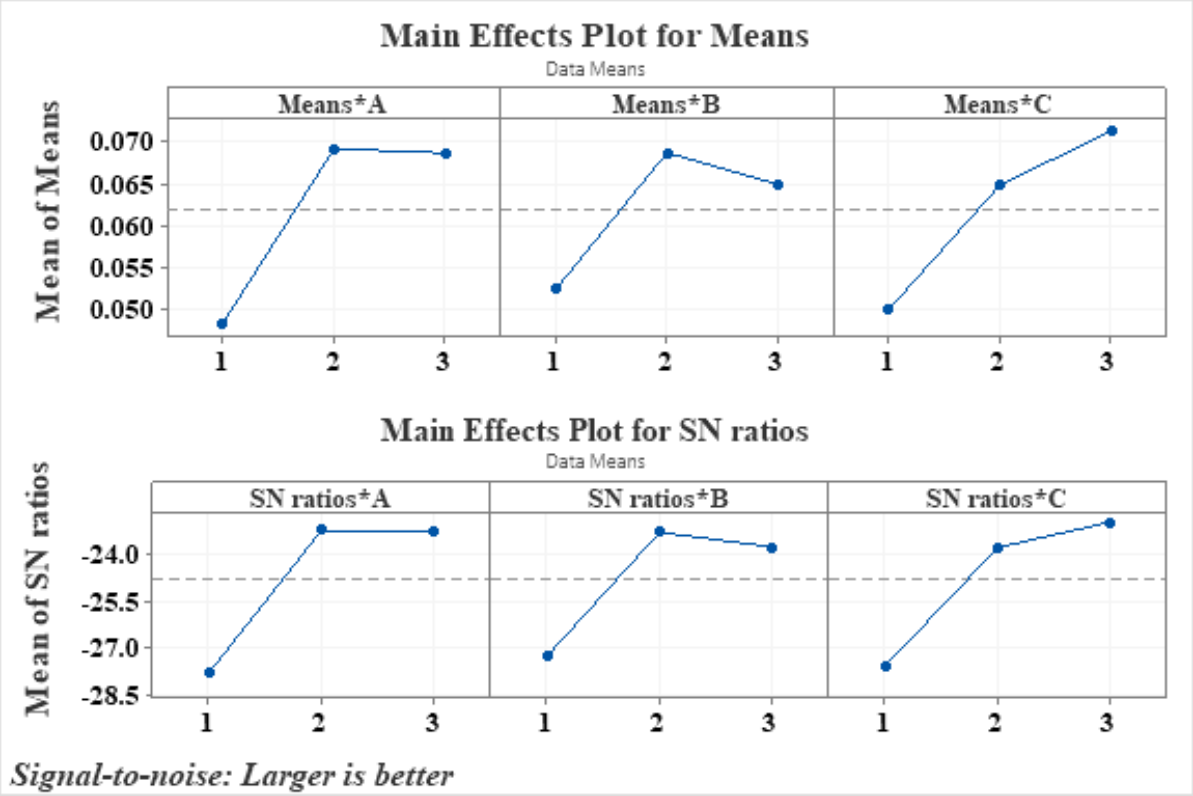

Figure 6: Main effect plot for means and SN ratios for proposed SMR.

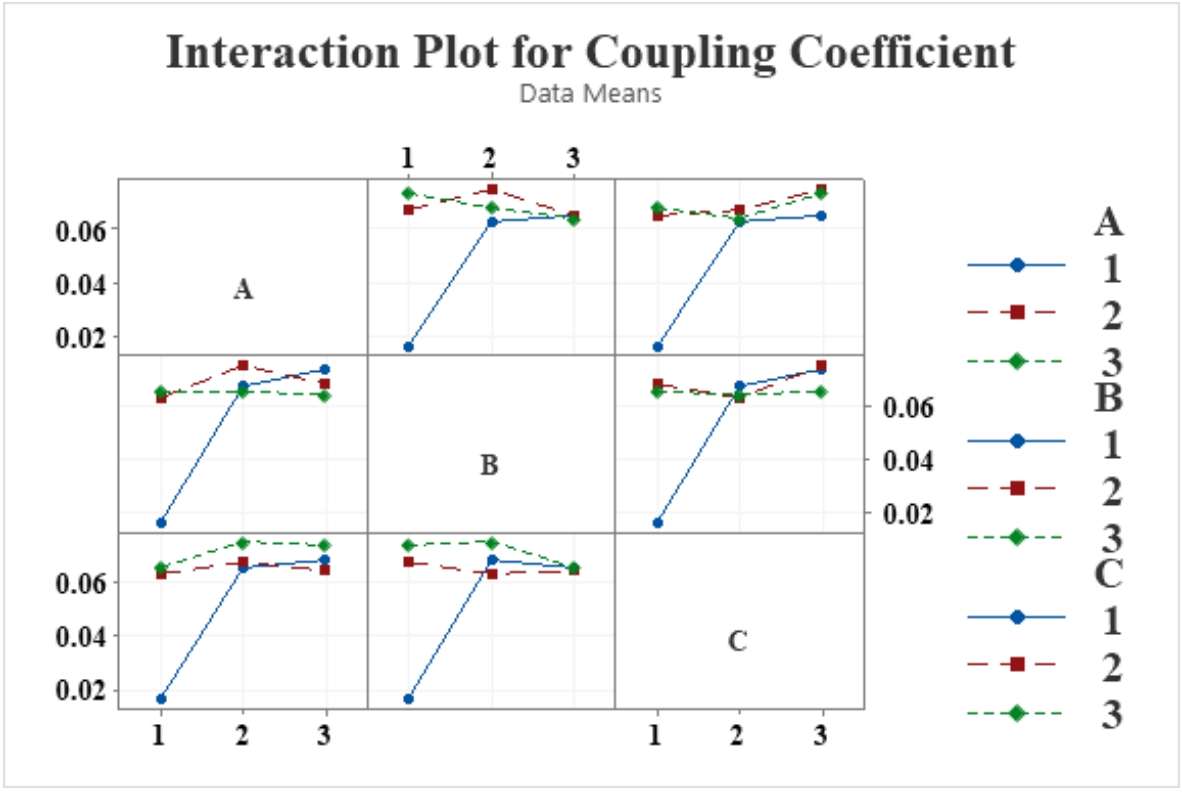

Figure 7: Interaction plot for proposed SMR sensor output parameter.

Figure 6 shows the main effect plot for means and SN Ratios obtained from Taguchi DoE analysis using Minitab 19 Software, respectively. Figure 6 also describes the effect of various levels of control factors on coupling coefficient. From the curve it can be said that for control factor C (sensing Layer Thickness) Level 3 have significant effect on designing of FBAR sensor whereas Level 2 of control factor A and B is demonstrating dominant effect in the design of FBAR sensor. Interaction plots of various control factors are shown in figure 7.

Table 8: Analysis of Variance

Factor	DoF	Sum of Squares	Mean of Squares	F-Value	P-Value
A	2	0.000850	0.000425	1.84	0.352
B	2	0.000432	0.000216	0.94	0.516
C	2	0.000718	0.000359	1.56	0.391
Error	2	0.000461	0.000231		
Total	8	0.002461			

From Table 8, Analysis of Variance, it is evident that factor A is responsible for 1.84/(1.84+0.94+1.56) =42.40 % percent of variation of coupling coefficient. Similarly, effect of the factors B and C have been calculated and it is observed that overall impact of Factors B and C on coupling coefficient is21.66% and 37.94%, respectively.

Table 9: Optimized Dimensions for SMR sensor

Layer	Layer Material	Optimized Thickness (μm)
Electrodes	Al	0.2
Piezoelectric Layer	ZnO	2
Insulating Layer	SiO2	0.3
Low Acoustic Impedance Layer	SiO2	1.028
High Acoustic Impedance Layer	Mo	1.008
Sensing Layer	PIB	0.68

The optimized dimensions of proposed SMR structure are tabulated in Table 9. Finally, optimized SMR structure has been simulated in COMSOL Multiphysics software. Figure 8, shows the mesh view of optimized device. Figure 9, shows resonance characteristics of the resonator. The resonant and anti-resonant frequencies, extracted from Figure 9, are 1.359 GHz and 1.402 GHz, respectively. The value of Quality factor (Q) can be obtained from Figure 10.

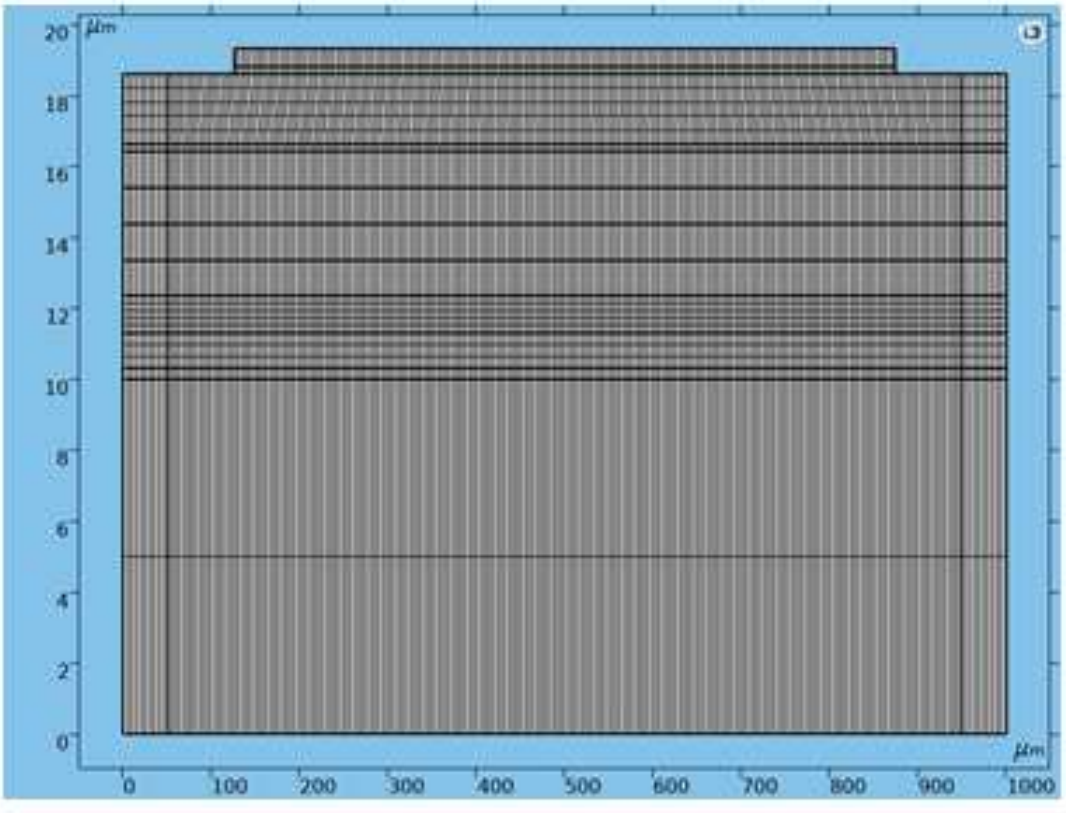

Figure 8: Mesh view of optimized SMR.

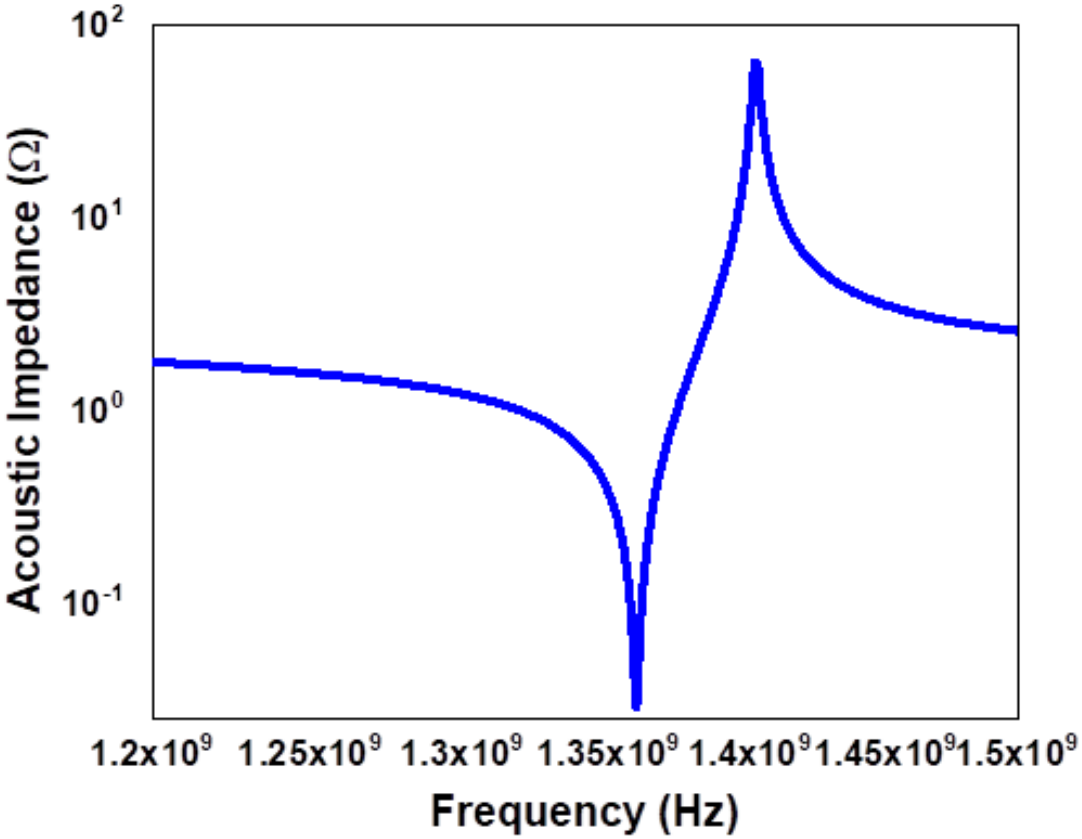

Figure 9: Acoustic impedance v/s frequency plot for optimized SMR.

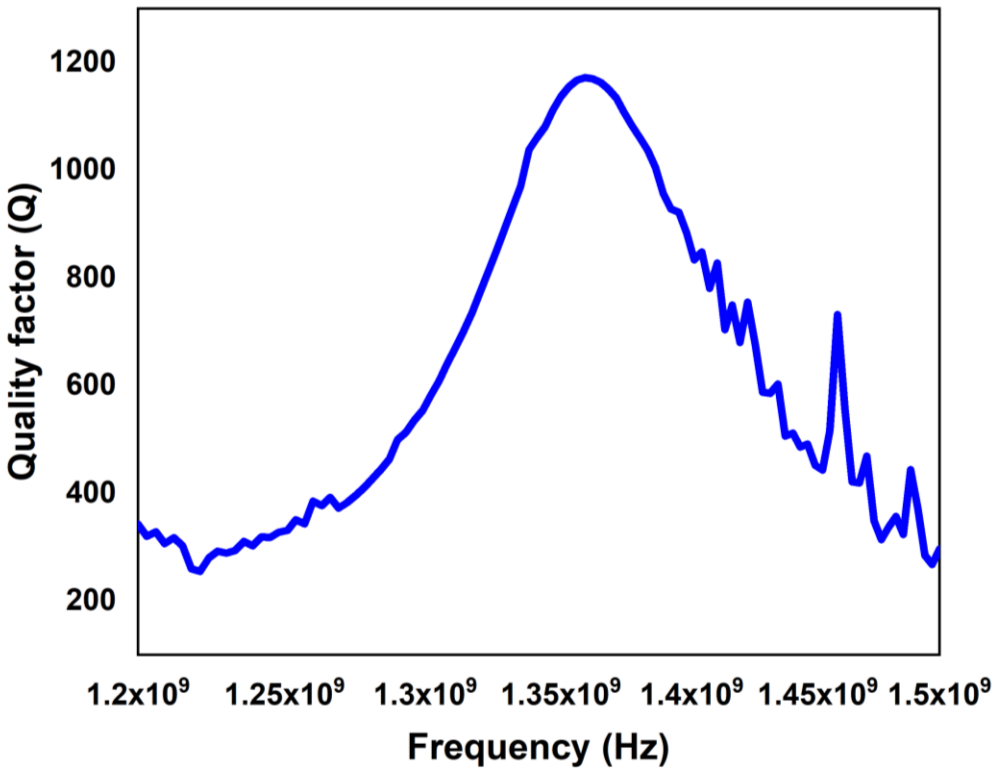

Figure 10: Quality factor v/s frequency plot for optimized SMR.

The simulated value of coupling coefficient, Quality factor and figure of merit (FoM) are 0.075596(or 7.5596%), 1171 and ≈88, respectively. The value of coupling coefficient can be calculated by substituting the value of resonant and anti-resonant frequencies to equation (8) whereas the FoM can be calculated by

$$FoM = K_{eff}^2 . \mathrm{Q} \qquad (12)$$

Where K_{eff}^2 and Q denotes the coupling coefficient and Quality Factor, respectively.

Table 10: Comparison of proposed SMR with existing literature

S.No.	Device Type	Quality Factor (Q)	Coupling coefficient (K_{eff}^2)	FoM	Reference
1.	Solidly Mounted FBAR	1855	0.024800	46.0040	[33]
2.	Solidly Mounted FBAR	832 457	0.036900 0.037700	30.7008 17.9050	[34]
3.	Solidly Mounted FBAR	746	0.029451	21.9700	[35]
4.	Solidly Mounted FBAR	414 523	0.056000 0.039000	23.1840 20.3970	[36]
5.	Solidly Mounted FBAR	201	0.043200	8.6900	[37]
6.	Solidly Mounted FBAR	312	0.017000	5.3040	[38]
7.	Solidly Mounted FBAR	450	0.051400	23.1300	[39]
8.	Solidly Mounted FBAR	758	0.073600	55.7888	[15]
9.	**Solidly Mounted FBAR**	**1171**	**0.075596**	**88.5229**	**Present work**

Proposed sensor performance is compared with existing literature and summarized in Table 10. It is evident from the table that proposed optimized SMR possess best performance as compared to others in terms of coupling coefficient and FoM.

Conclusions

Taguchi Design of Experiments (DoE) and ANOVA (Analysis of Variance) methods have been utilized to find the optimal combinations and to analyze the effect of individual layer thickness on SMR sensor performance. The optimum combination of various parameters has been used to predict the performance of SMR and same has been validated through the finite element modeling (FEM) simulation. The optimization has been done to achieve enhancement in coupling coefficient of SMR sensor. The best optimized values obtained for the thickness of metal electrodes, piezoelectric, sensing, insulation, low and high acoustic impedance layers have been found to be 0.2 µm, 2µm, 0.68 µm, 0.3 µm, 1.028 µm and1.008 µm, respectively. The results of the present study show that for the optimized dimension of SMR structure, simulated values of coupling coefficient (K_{eff}^2), Quality factor (Q) and figure of merit (FoM) are 0.075596 (or 7.5596%), 1171.6 and ≈ 88, respectively. Optimized structure performance has been compared with existing SMR sensors and it is observed that proposed SMFAR exhibits performance enhancement in terms of FoM by ≈37 %.

Acknowledgement

The author would like to acknowledge the support of the Ministry of Electronics and Information Technology (MeitY), Government of India for providing fellowship grant under Visvesvaraya PhD Scheme for Electronics and IT. The authors also acknowledge support of Material Research Centre (MRC), Malaviya National Institute of Technology Jaipur, for providing the simulation facilities.

Conflict of Interest

The authors declare that they have no conflict of interest.

References

[1] Fu, Y.Q., Luo, J.K., Nguyen, N.T., Walton, A.J., Flewitt, A.J., Zu, X.T., Li, Y., McHale, G., Matthews, A., Iborra, E. and Du, H., 2017. Advances in piezoelectric thin films for acoustic biosensors, acoustofluidics and lab-on-chip applications. *Progress in Materials Science*, *89*, pp.31-91.

[2] Larson, J.D., Bradley, P.D., Wartenberg, S. and Ruby, R.C., 2000, October. Modified Butterworth-Van Dyke circuit for FBAR resonators and automated measurement system. In *2000 IEEE Ultrasonics Symposium. Proceedings. An International Symposium (Cat. No. 00CH37121)* (Vol. 1, pp. 863-868). IEEE.

[3] Tadigadapa, S. and Mateti, K., 2009. Piezoelectric MEMS sensors: state-of-the-art and perspectives. *Measurement Science and technology*, *20*(9), p.092001.

[4] Lakin, K.M. and Wang, J.S., 1980, November. UHF composite bulk wave resonators. In *1980 Ultrasonics Symposium* (pp. 834-837). IEEE.

[5] Löbl, H.P., Klee, M., Milsom, R., Dekker, R., Metzmacher, C., Brand, W. and Lok, P., 2001. Materials for bulk acoustic wave (BAW) resonators and filters. *Journal of the European Ceramic Society*, *21*(15), pp.2633-2640.

[6] Lu, Y., Emanetoglu, N.W. and Chen, Y., 2006. ZnO piezoelectric devices. In *Zinc Oxide Bulk, Thin Films and Nanostructures* (pp. 443-489). Elsevier Science Ltd.

[7] Jose, S., 1980. *Reflector stack optimization for Bulk Acoustic Wave resonators* (Vol. 37, pp. 993-995).

[8] Johar, A.K., Varma, T., Periasamy, C., Agarwal, A. and Boolchandani, D., 2020. Design, Analysis and Finite Element Modeling of Solidly Mounted Film Bulk Acoustic Resonator for Gas Sensing Applications. *Journal of Electronic Materials*, *49*(2), pp.1503-1511.

[9] Villa-López, F.H., Rughoobur, G., Thomas, S., Flewitt, A.J., Cole, M. and Gardner, J.W., 2015. Design and modelling of solidly mounted resonators for low-cost particle sensing. *Measurement Science and Technology, 27(2), p.025101.*

[10] Wingqvist, G., Bjurström, J., Liljeholm, L., Yantchev, V. and Katardjiev, I., 2007. Shear mode AlN thin film electro-acoustic resonant sensor operation in viscous media. *Sensors and Actuators B: Chemical*, *123*(1), pp.466-473.

[11] Mai, L., Pham, V.S. and Yoon, G., 2009. ZnO-based film bulk acoustic resonator devices on a specially designed Bragg reflector. *Applied Physics A*, *95*(3), pp.667-671.

[12] Yan, Z., Zhou, X.Y., Pang, G.K.H., Zhang, T., Liu, W.L., Cheng, J.G., Song, Z.T., Feng, S.L., Lai, L.H., Chen, J.Z. and Wang, Y., 2007. ZnO-based film bulk acoustic resonator for high sensitivity biosensor applications. *Applied physics letters*, *90*(14), p.143503.

[13] Qiu, X., Oiler, J., Zhu, J., Wang, Z., Tang, R., Yu, C. and Yu, H., 2010. Film bulk acoustic-wave resonator based relative humidity sensor using ZnO films. *Electrochemical and Solid State Letters, 13(5), p.J65.*

[14] Di Pietrantonio, F., Benetti, M., Cannata, D., Verona, E., Palla-Papavlu, A., Dinca, V., Dinescu, M., Mattle, T. and Lippert, T., 2012. Volatile toxic compound detection by surface acoustic wave sensor array coated with chemoselective polymers deposited by laser induced forward transfer: Application to sarin. *Sensors and Actuators B: Chemical*, *174*, pp.158-167.

[15] Johar, A.K., Patel, R., Periasamy, C., Agarwal, A. and Boolchandani, D., 2018. FEM modeling and simulation of SMFBAR sensor with PIB as sensing layer for tetrachloroethane (PCE) gas detection. *Materials Research Express*, *6*(1), p.015033.

[16] Tay, K.W., Huang, C.L. and Wu, L., 2004. Influence of piezoelectric film and electrode materials on film bulk acoustic-wave resonator characteristics. *Japanese journal of applied physics*, *43*(3R), p.1122.

[17] Weber, J., Albers, W.M., Tuppurainen, J., Link, M., Gabl, R., Wersing, W. and Schreiter, M., 2006. Shear mode FBARs as highly sensitive liquid biosensors. *Sensors and Actuators A: Physical*, *128*(1), pp.84-88.

[18] Goel, R., Chechi, R. and Chawla, P., Design the Film Bulk Acoustic Resonator (FBAR) Filter for Wireless Applications.

[19] Yang, C.M., Uehara, K., Kim, S.K., Kameda, S., Nakase, H. and Tsubouchi, K., 2003, October. Highly c-axis-oriented AlN film using MOCVD for 5GHz-band FBAR filter. In *IEEE Symposium on Ultrasonics, 2003* (Vol. 1, pp. 170-173). IEEE.

[20] Reddy, P.R. and Mohan, B.C., 2012. Design and analysis of film bulk acoustic resonator (FBAR) filter for RF applications. *International Journal of Engineering Business Management*, 4, p.28.

[21] Ruby, R., 2007, October. 11E-2 review and comparison of bulk acoustic wave FBAR, SMR technology. In *2007 IEEE Ultrasonics Symposium Proceedings* (pp. 1029-1040). IEEE.

[22] Zhang, Y. and Chen, D., 2012. *Multilayer integrated film bulk acoustic resonators*. Springer Science & Business Media.

[23] Bjurström, J., Wingqvist, G., Yantchev, V. and Katardjiev, I., 2007. Temperature compensation of liquid FBAR sensors. *Journal of Micromechanics and Microengineering, 17(3), p.651.*

[24] Tay, K.W., Huang, C.L. and Wu, L., 2004. Influence of piezoelectric film and electrode materials on film bulk acoustic-wave resonator characteristics. *Japanese journal of applied physics*, *43*(3R), p.1122.

[25] Campanella, H., 2010. *Acoustic wave and electromechanical resonators: concept to key applications*. Artech House.

[26] Chi, H.W. and Bloebaum, C.L., 1996. Mixed variable optimization using Taguchi's orthogonal arrays. *Structural optimization*, 12(2-3), pp.147-152.

[27] Kharisma, A., Murphiyanto, R.D.J., Perdana, M.K. and Kasih, T.P., 2017, December. Application of Taguchi method and ANOVA in the optimization of dyeing process on cotton knit fabric to reduce re-dyeing process. *In IOP Conference Series: Earth and Environmental Science (Vol. 109, No. 1, p. 012023). IOP Publishing.*

[28] Balavalad, Kirankumar and Sheeparamatti, Basavaprabhu. 2017. Optimum Combination and Effect Analysis of Piezoresistor Dimensions in Micro Piezoresistive Pressure Sensor Using Design of Experiments and ANOVA: a Taguchi Approach. *Sensors and Transducers*. 211. 14-21.

[29] Sharma, G.K., Johar, A.K., Kumar, T.B. and Boolchandani, D., 2020. Effectiveness of Taguchi and ANOVA in design of differential ring oscillator. *Analog Integrated Circuits and Signal Processing*, pp.1-11.

[30] Kumar, T.B., Panda, A., Sharma, G.K., Johar, A.K., Kar, S.K. and Boolchandani, D., 2020. Taguchi DoE and ANOVA: A systematic perspective for performance optimization of cross-coupled channel length modulation OTA. *AEU-International Journal of Electronics and Communications*, *116*, p.153070.

[31] Deng, X., Wang, S., Youssef, H., Qian, L. and Liu, Y., 2020. Study on the influence of key design parameters on lubrication characteristics of a novel gear system applying Taguchi method. *Structural and Multidisciplinary Optimization*, pp.1-15.

[32] Fattinger, G.G., TriQuint Semiconductor Inc, 2013. *Bulk acoustic wave devices and method for spurious mode suppression*. U.S. Patent 8,456,257.

[33] Hui, Y., Qian, Z. and Rinaldi, M., 2013, July. A 2.8 GHz combined mode of vibration aluminum nitride MEMS resonator with high figure of merit exceeding 45. In *2013 Joint European Frequency and Time Forum & International Frequency Control Symposium (EFTF/IFC)* (pp. 930-932). IEEE.

[34] Lee, S.H., Yoon, K.H. and Lee, J.K., 2002. Influence of electrode configurations on the quality factor and piezoelectric coupling constant of solidly mounted bulk acoustic wave resonators. *Journal of Applied Physics*, *92*(7), pp.4062-4069.

[35] Mansour, A.A. and Kalkur, T.S., 2016. High-Quality-Factor and Low-Temperature-Dependence SMR FBAR Based on BST Using MOD Method. *IEEE transactions on ultrasonics, ferroelectrics, and frequency control*, *64*(2), pp.452-462.

[36] Lanz, R. and Muralt, P., 2003, October. Solidly mounted BAW filters for 8 GHz based on AlN thin films. In *IEEE Symposium on Ultrasonics, 2003* (Vol. 1, pp. 178-181). IEEE.

[37] Lee, J.B., Kim, H.J., Kim, S.G., Hwang, C.S., Hong, S.H., Shin, Y.H. and Lee, N.H., 2003. Deposition of ZnO thin films by magnetron sputtering for a film bulk acoustic resonator. *Thin Solid Films*, *435*(1-2), pp.179-185.

[38] Link, M., Schreiter, M., Weber, J., Primig, R., Pitzer, D. and Gabl, R., 2006. Solidly mounted ZnO shear mode film bulk acoustic resonators for sensing applications in liquids. *IEEE transactions on ultrasonics, ferroelectrics, and frequency control*, *53*(2), pp.492-496.

[39] Knapp, M., Hoffmann, R., Lebedev, V., Cimalla, V. and Ambacher, O., 2018. Graphene as an active virtually massless top electrode for RF solidly mounted bulk acoustic wave (SMR-BAW) resonators. *Nanotechnology, 29(10), p.105302.*